GU J Sci 31(1): 82-98 (2018)

Gazi University

Journal of Science

http://dergipark.gov.tr/gujs

Genetic Algorithm and Fuzzy Based on The Taguchi Optimization to Improve The Torque Behavior of An Outer-Rotor Permanent-Magnet Machine

Yusuf ÖZOĞLU[1,*]

[1]*Istanbul University, Vocational School of Technical Science, Istanbul, Turkey.*

Article Info

Received: 24/04/2017
Accepted: 12/02/2018

Keywords

Outer-Rotor Permanent-Magnet Machine,
Torque Ripple,
Taguchi Method,
Fuzzy Inference System,
Multi-Response Performance Index,
Genetic Algorithm.

Abstract

The torque behavior of an outer-rotor surface-mounted permanent-magnet machine is improved by identifying seven pertinent design variables, including rotor height. The optimal design variables are revealed by analyzing 18 experiments determined by the Taguchi method for the minimum torque ripple, minimum total harmonic distortion of the induced voltage, and maximum average torque. In addition, the optimal design variables are obtained very quickly by using fuzzy inference mechanism and genetic algorithm (GA) based on the Taguchi method with the single response of the multi-response performance index instead of multiple responses. A considerable amount of multi-response improvement is achieved according to the results of the two optimizations.

1. INTRODUCTION

Recently, considerable interest has arisen in permanent-magnet synchronous machines (PMSMs) that have no rotor windings, resulting in lower copper losses. However, PMSMs suffer from high torque ripple, cogging torque, and large unbalanced magnetic forces. There has been much research on slot and permanent-magnet (PM) designs. These include designing the slot opening to minimize the torque ripple [1], studying the influence of slot-opening width, pole-arc coefficient, magnet thickness, and air-gap size on electromotive force (EMF) harmonics [2], varying the width of the magnet poles to minimize the cogging torque [3], showing the significant effects of pole-arc coefficient, eccentricity, and magnet shape on the harmonic content and cogging torque [4], increasing the PM offset without significant reduction in back EMF and motor efficiency [5], and determining the optimal split ratio for an external-rotor PMSM [6].

Some studies have used the Taguchi method. These include maximizing output power and efficiency [7], optimizing average torque, torque ripple, and the ratio of torque ripple to average torque [8], considering the manufacturing tolerances of PM in the interior PMSM for a robust design of the EMF characteristic analysis [9], minimizing the cogging torque and maximizing the efficiency [10]. In the following studies, the Taguchi method and the fuzzy inference system are used together. These incorporate optimizing cogging torque and efficiency [11], optimizing torque ripple, efficiency, and torque-to-magnet-volume ratio [12], optimizing efficiency and average torque to torque ripple factor [13].

Some other studies in the literature are based on genetic algorithm. An optimization technique based on GAs has been developed and applied to design of SPM motors [14], optimization of cogging torque and efficiency was examined using the Taguchi method with genetic algorithms [15], a Strength Pareto

*Corresponding author, e-mail: yozoglu@istanbul.edu.tr

Evolutionary Algorithm is developed for in-wheel SPM [16], maximizing output torque while minimizing the torque ripple was demonstrated the use of both genetic algorithm and Taguchi's technique [17], and a hybrid optimization scheme using GA in conjunction with Kriging were proposed for optimizing rotor of interior PMSM [18], the minimal cost design of an Axial Flux PMG was searched by using a GA [19].

Most studies do not discuss the effect of design parameters on the torque behavior. However, it is important to determine the design variables that will be used in the optimization process. The primary focus of the present study is the effect of design parameters on the torque behavior of a surface-mounted permanent magnet (SPM) machine. The optimal range of design parameters is determined before the optimization process. In addition, the main dimensions of an SPM machine (i.e., the stator and rotor heights) were not considered in above studies. Hence, the present study considers the effects of stator and rotor height on the torque behavior. Seven design variables, including the rotor height, are considered here.

A different set of optimal levels must be obtained for each response (average torque, torque ripple, and total harmonic distortion (THD)) to determine the optimal levels of design parameters based on a single response in a multi-response problem. Unlike the literature, both the fuzzy inference system and the genetic algorithm are used with the Taguchi method to combine the multiple responses into a single response in this study.

2. FINITE ELEMENT ANALTSIS OF OR-SPM MACHINE

2.1. Design Parameters

In this study, an SPM machine with an outer rotor (OR) is selected for study. The geometry of this OR-SPM machine is shown in Figure 1, and its performance parameters are given in Table 1. These values are used as the multiple response/performance characteristics of the optimization process.

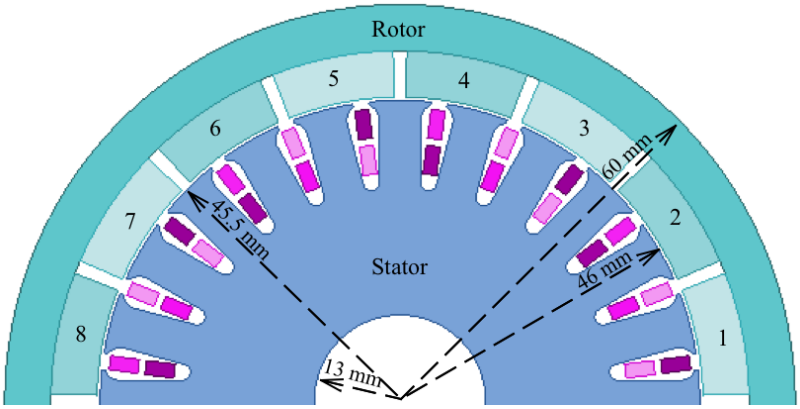

Figure 1. *Outer-rotor surface-mounted permanent-magnet (OR-SPM) machine*

The important performance values that were obtained by simulating the OR-SPM machine as a two-dimensional finite-element model are given in Table 2 as reference performance values that are used for comparison with the optimization results. k_{w1} and q are the fundamental winding factor and the value of slot/pole/phase and the pole number, respectively.

Previous studies have tended to overlook the effect of design parameters such as the stator and rotor heights, slot opening, and magnet dimensions on the torque behavior. Hence, the primary goal here is to improve the torque behavior of the OR-SPM machine under consideration by focusing on the influence of such design parameters. The relevant design parameters are the stator height (H_s), the rotor height (H_r), the air-gap length (g), the magnet embrace (E_m), the magnet thickness (T_m), the magnet offset (O_m), the slot-opening width (b_{s0}), and the slot-opening height (h_{s0}). All these design parameters are marked on the geometry of the OR-SPM machine shown in Figure 2, and their reference values are given in Table 1.

Table 1. *Reference parameters of the OR-SPM machine*

Parameter	Value
Inner & Outer Diameter of Rotor	92-120 mm
Inner & Outer Diameter of Stator	26-91 mm
Height of Stator & Rotor (H_s, H_r)	32.5-14 mm
Stack Length	65 mm
Embrace of Magnet (E_m)	0.9
Offset of Magnet (O_m)	0 mm
Thickness of Magnet (T_m)	7 mm
Slot Opening Height & Width (h_{s0}, b_{s0})	0.5-2.5 mm
Slot Body Height & Bottom Width	9.48-2.5 mm
Slot Wedge Width	5 mm
Slot and Pole Number	24s-16p
Rated Output Power	0.55 kW
Rated Voltage	220 V
Rated speed	1500 rpm
Material of Steel	M19-24G
Material of Magnet	XG196/96

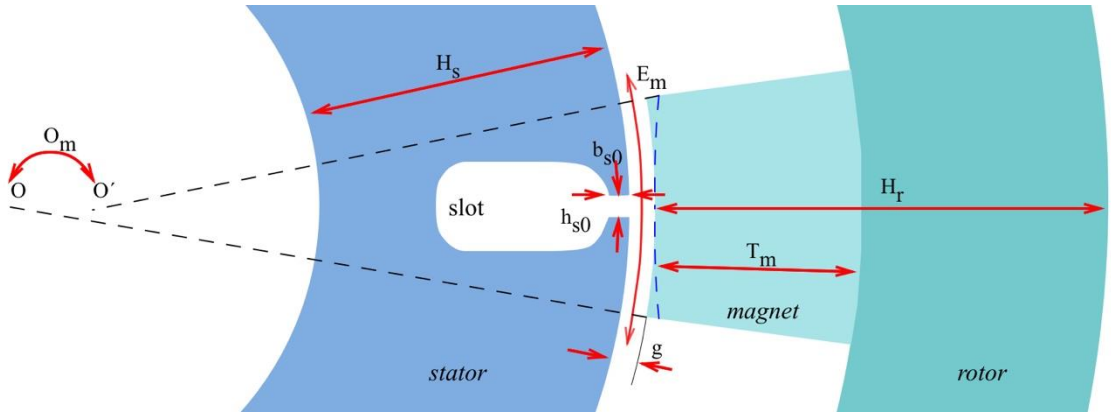

Figure 2. *Design parameters for the OR-SPM machine*

2.2. Torque Performance Corresponding to Design Parameters

The important performance values that were obtained by simulating the OR-SPM machine as a two-dimensional finite-element model are given in Table 2 as reference performance values that are used for comparison with the Optimization results.

Table 2. *Reference performance characteristics*

Slot/Pole	q	k_{w1}	T_{avg} (Nm)	T_{rip} (%)	THD (%)
24/16	0.5	0.866	12.55	5.17	1.63

The torque ripple (T_{rip}) is defined as

$$T_{rip} = \frac{T_{rms}}{T_{avg}} \times 100\% \tag{1}$$

where T_{rms} and T_{avg} are the root-mean-square of ripple component and average values, respectively, of the instantaneous torque.

The variations in the average torque and the torque ripple with each of the design parameters were obtained by analyzing the finite-element model. The outer diameter of the OR-SPM machine was kept constant during this process. These variations are shown in Figure 3. The torque behavior (i.e., the average torque and the torque ripple) is extremely sensitive to each of the design parameters, except for the stator height. Hence, the stator height was excluded as a design variable for the optimization process. The smallest value of the stator height (H_s = 18 mm) is used as the optimal value so that the magnetic field does not exceed the limit value in the stator yoke. Hence, its reference value (32.5 mm) was accepted as the optimal value of 18mm. The other design parameters are accepted as variables in the optimization process because of their torque sensitivity.

The optimal range of each design parameter was determined for the reference boundary of the magnetic flux density. Thus, the first step in the process was the determination of the design parameters and their optimal ranges for use in the optimization. Their optimal ranges providing the best torque behavior are determined by observing the variations in the average torque and the torque ripple in Figure 3. These optimal ranges are H_r = 12–14 mm, g = 0.45–0.55 mm, E_m = 0.88–0.90, T_m = 8–10 mm, O_m = 12–16 mm, b_{s0} = 2.6–2.8 mm, and h_{s0} = 0.4–0.6 mm.

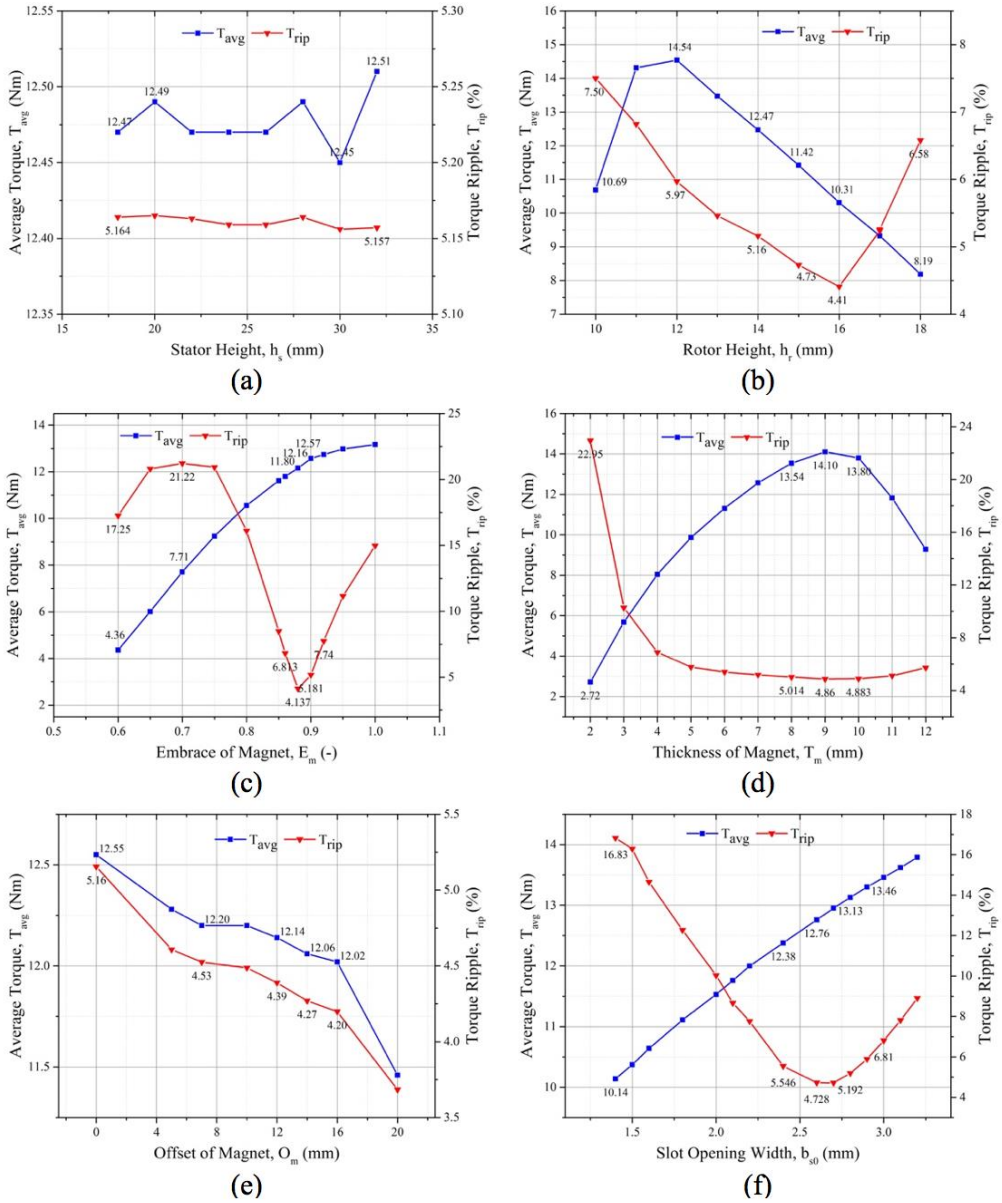

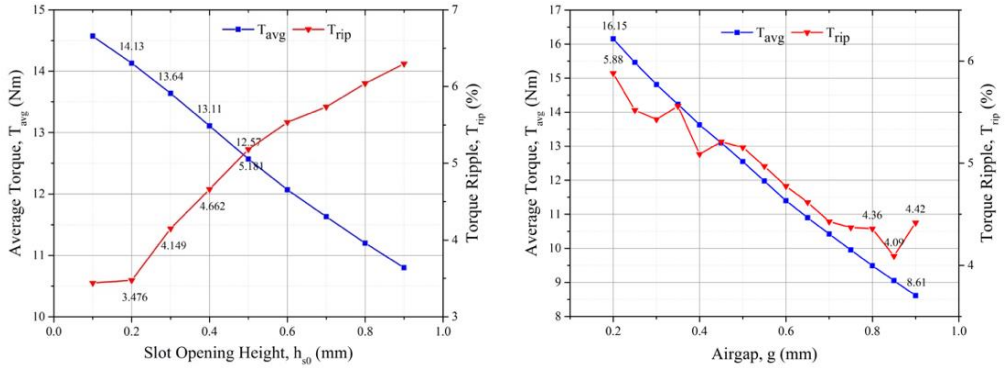

Figure 3. *Variations in average torque (blue) and torque ripple (red) with a) stator height b) rotor height c) magnet embrace d) magnet thickness e) magnet offset f) slot-opening width g) slot-opening height h) air-gap length*

3. OPTIMIZATION WITH THE TAGUCHI METHOD

The multi-parameter Taguchi method provides the designer with an efficient approach for doing experiments to determine near-optimal parameter values. The process diagram of the system to be optimized is shown in Figure 4. This process transforms some input/signal factors (M) into an output that has one or more observable response variables (Y). The control factors (X) are controllable, whereas the noise factors (Z) are uncontrollable. The function of the system can be shown in terms of its process diagram, which reflects the output (Y) as a result of the input (M) and other influencing factors (X, Z) on the system [20].

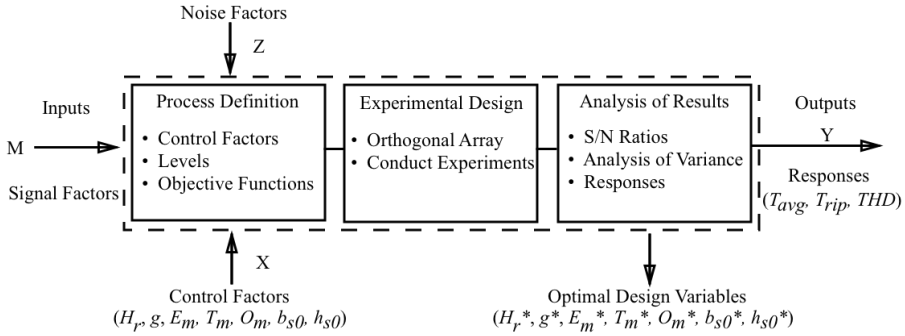

Figure 4. *Process diagram of system*

The relevant factors are the variables that have a direct influence on the performance of the process. The levels are the values that define the conditions of the factors that are held during the experiments. An orthogonal array (OA) is used to design the experiments and describe the trial conditions [20].

The signal-to-noise (S/N) ratio measures how the response varies relative to the target. To achieve an optimally designed product, two different S/N ratios are calculated using Eqs. 2 and 3. If the goal is to maximize the response, the S/N ratio is taken as "larger is better" (LIB) and is defined as

$$S/N = -10\log_{10}\left[\frac{1}{n}\sum_{i=1}^{n}\frac{1}{y_i^2}\right] \tag{2}$$

If the goal is to minimize the response, the S/N ratio is taken as "smaller is better" (SIB) and is defined as

$$S/N = -10\log_{10}\left[\frac{1}{n}\sum_{i=1}^{n}y_i^2\right] \tag{3}$$

where n is the number of experiments for each object function and y_i is the value of the experiment's response.

3.1 Application of The Taguchi Method

Primarily, an experiment to study above factors is accomplished by using an $L18$ array as shown below:

$$L_n\left(i^x\right) = L_{18}\left(2^1 3^6\right) = L18 \tag{4}$$

where n, i, and x are the number of experiments, the number of levels, and the number of control factors, respectively.

The design consists of one factor at two levels and six factors at three levels each (Table 3). There are seven control factors (A–G), one of which has two levels and the others have three levels in this optimization problem. These control factors are also known as the design variables. The $L18$ response values are tabulated in Table 4.

Table 3. *Design variables and levels*

Design Variables		**Level 1**	**Level 2**	**Level 3**
E_m	A	0.88	0.9	-
T_m	B	8	9	10
O_m	C	12	14	16
H_r	D	12	13	14
b_{s0}	E	2.6	2.7	2.8
h_{s0}	F	0.4	0.5	0.6
g	G	0.45	0.5	0.55

Table 4. *Results/responses of L18 orthogonal array*

n	**E_m**	**T_m**	**O_m**	**H_r**	**b_{s0}**	**h_{s0}**	**g**	**T_{avg}**	**T_{rip}**	**THD**
	A	**B**	**C**	**D**	**E**	**F**	**G**	**(Nm)**	**(%)**	**(%)**
1	0.88	8	12	12	2.6	0.4	0.45	15.27	3.38	1.25
2	0.88	8	14	13	2.7	0.5	0.5	14.11	4.18	1.19
3	0.88	8	16	14	2.8	0.6	0.55	12.21	5.98	1.15
4	0.88	9	12	12	2.7	0.5	0.55	11.21	5.35	1.28
5	0.88	9	14	13	2.8	0.6	0.45	14.35	5.06	1.16
6	0.88	9	16	14	2.6	0.4	0.5	14.05	3.57	1.19
7	0.88	10	12	13	2.6	0.6	0.5	11.14	4.97	1.27
8	0.88	10	14	14	2.7	0.4	0.55	13.61	4.39	1.19
9	0.88	10	16	12	2.8	0.5	0.45	8.72	9.59	1.32
10	0.9	8	12	14	2.8	0.5	0.5	13.64	4.35	1.41
11	0.9	8	14	12	2.6	0.6	0.55	13.19	4.53	1.47
12	0.9	8	16	13	2.7	0.4	0.45	15.56	3.47	1.39
13	0.9	9	12	13	2.8	0.4	0.55	14.47	3.85	1.40
14	0.9	9	14	14	2.6	0.5	0.45	14.46	3.54	1.44
15	0.9	9	16	12	2.7	0.6	0.5	11.22	4.93	1.45
16	0.9	10	12	14	2.7	0.6	0.45	13.90	3.97	1.50
17	0.9	10	14	12	2.8	0.4	0.5	8.89	7.23	1.56
18	0.9	10	16	13	2.6	0.5	0.55	11.22	4.08	1.45

The LIB case is related to the objective function of the average torque. The SIB case is related to the objective function of the torque ripple, and to the THD of the back-EMF; minimizing the THD is the second main goal of this study. The quality characteristics of the average torque, torque ripple, and back-EMF THD as calculated by the S/N ratio are given in Tables 5, respectively. In addition, Figure 5 show the main-effect plots for the S/N ratio according to each design variable.

Table 5. *Average torque, torque ripple and THD of back-EMF for the design variables.*

T_{avg}

Level	A	B	C	D	E	F	G
i=1	12.74	14.00	13.27	11.42	13.22	13.64	13.71
i=2	12.95	13.29	13.10	13.48	13.27	12.23	12.17
i=3	-	11.25	12.16	13.65	12.05	12.67	12.65
LIB	A2	B1	C1	D3	E2	F1	G1

T_{rip}

Level	A	B	C	D	E	F	G
i=1	5.16	4.32	4.31	5.84	4.01	4.32	4.84
i=2	4.44	4.38	4.82	4.27	4.38	5.18	4.87
i=3	-	5.71	5.27	4.30	6.01	4.91	4.70
SIB	A2	B1	C1	D2	E1	F1	G3

THD

Level	A	B	C	D	E	F	G
i=1	1.22	1.31	1.35	1.39	1.35	1.33	1.34
i=2	1.45	1.32	1.34	1.31	1.33	1.35	1.35
i=3	-	1.38	1.33	1.31	1.33	1.33	1.32
SIB	A1	B1	C3	D23	E23	F13	G3

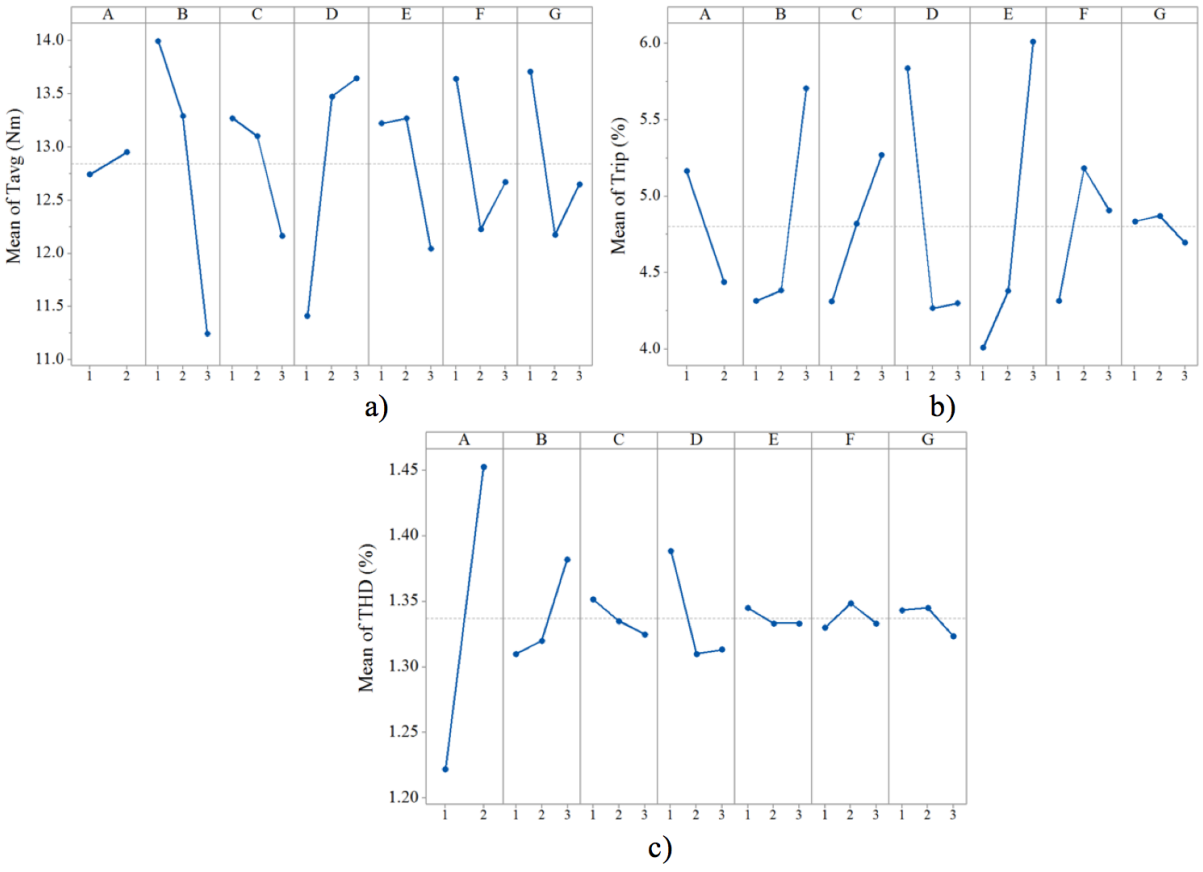

Figure 5. *Effect of main design variables on a) average torque T_{avg} b) torque ripple T_{rip} c) back-EMF THD*

Analysis of variance does not analyze the optimization problem directly, but rather it extracts the relative importance of the design variables. To evaluate the significant effect of the design variables on the responses, the sum of squares (SS) due to various design variables can be calculated by

$$SS_A = 3\sum_{i=1}^{3}\left(m_{A_i} - m\right)^2 \tag{5}$$

The SS for the other seven variables (SS_B, SS_C, and so on) can be obtained in the same way.

Table 6. *Significant effects of the design variables*

Factors		**T_{avg} (Nm)**		**T_{rip} (%)**		**THD (%)**	
		SS	Effect Ratio (%)	SS	Effect Ratio (%)	SS	Effect Ratio (%)
E_m	A	0.20	0.3	2.36	5.8	0.24	82.4
T_m	B	24.49	34.9	7.37	18.2	0.02	6.3
O_m	C	4.28	6.1	2.76	6.8	0.00	0.8
H_r	D	18.46	26.3	9.62	23.8	0.02	8.1
b_{s0}	E	5.75	8.2	13.56	33.5	0.00	0.2
h_{s0}	F	6.29	9.0	2.35	5.8	0.00	0.4
g	G	7.41	10.6	0.10	0.3	0.00	0.6

These results are summarized in Table 6. The magnet thickness (B) and rotor height (D) are revealed as the dominant design variables for the average torque. The slot-opening width (E), rotor height (D), and magnet thickness (B) stand out for the torque ripple. The magnet embrace (A) is revealed as the only dominant design variable for the THD.

3.2. Optimal Design Variables for Taguchi Analysis

From Tables 5, it is clear that the design-variable/level combination of A2-B1-C1-D3-E2-F1-G1 maximizes the average torque, A2-B1-C1-D2-E1-F1-G3 minimizes the torque ripple, and A1-B1-C3-D23-E23-F13-G3 minimizes the THD. From Table 6, the most influential design variables in relation to average torque, torque ripple, and THD are B-D, B-D-E, and A, respectively. It is primarily these variables that are evaluated.

Firstly, evaluation is performed in relation to average torque and torque ripple. The average torque is largest for B, D, and E, whereas the torque ripple is lowest. In addition, variables A, C, and F have the same effects on the average torque and the torque ripple. Variable G has a larger effect on the average torque than on the torque ripple. Therefore, the design variables A2, B1, C1, D23, E1, F1, and G1 are selected to constitute the maximum average torque and the minimum torque ripple.

In addition, design-variable A has a larger effect on the THD than on the average torque or the torque ripple. Thus, design-variable A2 can be replaced with A1. In this case, the THD decreases while the two torque values change. The optimal combination of design variables was determined as A12-B1-C1-D23-E1-F1-G1 for the maximum average torque, the minimum torque ripple, and the minimum THD.

Table 7. *Responses for the Taguchi analysis*

Model	**T_{avg} (Nm)**	**T_{rip} (%)**	**THD (%)**
1: A2-B1-C1-D2-E1-F1-G1	15.48	3.78	1.43
2: A2-B1-C1-D3-E1-F1-G1	14.36	3.65	1.44
3: A1-B1-C1-D2-E1-F1-G1	15.14	3.5	1.23
4: A1-B1-C1-D3-E1-F1-G1	14.02	3.61	1.24
Improvement in # 1	23.3%	-26.6%	-12.3%
Improvement in # 3	20.6%	-32.0%	-24.5%

The three optimal responses corresponding to the optimal design variables are given in Table 7. Four trials are available for two different values of A and D. When design-variable D varies from D2 to D3, the average torque decreases. Similarly, when design-variable A varies from A2 to A1, the THD decreases because A has a larger effect on the THD than on either of the two torque values. The improvements in the average torque, torque ripple, and THD are 20.6%, 32.0%, and 24.5%, respectively. Response #3 is more successful than #1 in terms of the torque ripple and the THD.

4. OPTIMIZATION WITH FUZZY INFERENCE SYSTEM

Fuzzy inference systems are also known as fuzzy-rule-based systems [21]. Basically, a fuzzy inference system is composed by five functional interfaces (Figure 6). The fuzzy-rule based system consists of fuzzification, inference engine, database base, rule base, and defuzzification interfaces. The fuzzification interface converts the inputs so that they can be interpreted and compared to the rules in the rule base. The rule base containing a number of fuzzy if-then rules. The database defines the membership function of the fuzzy sets used in the fuzzy rules. Mamdani fuzzy inference engine commonly used is based on the collection of fuzzy rules [22]. The defuzzification interface transforms the fuzzy result of inference into an output.

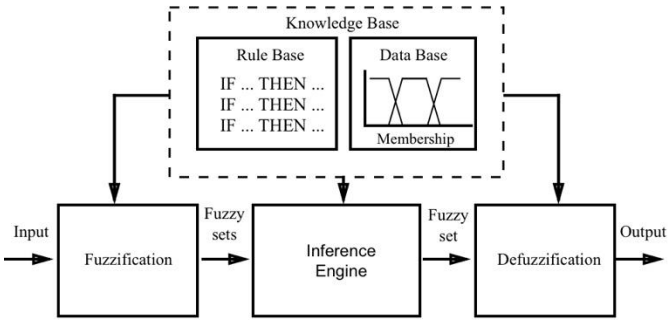

Figure 6. *Fuzzy inference system structure*

The rule base includes a group of if-then rules with for example, three inputs γ_1, γ_2 and γ_3, and one output η,

Rule 1: if γ_1 is A_1 and γ_2 is B_1 and γ_3 is C_1 then η is D_1

Rule 2: if γ_2 is A_2 and γ_2 is B_2 and γ_3 is C_2 then η is D_2

…

Rule n: if γ_1 is A_n and γ_2 is B_n and γ_3 is C_n then η is D_n

where A_i, B_i, C_i, and D_i are fuzzy sets defined by the corresponding membership functions, i.e. $\mu_{Ai}(\gamma_1)$, $\mu_{Bi}(\gamma_1)$, $\mu_{Ci}(\gamma_1)$ and $\mu_{Di}(\gamma_1)$.

The fuzzy reasoning of the rules provides a fuzzy output by using the max-min fuzzy interface operation. The membership function of the fuzzy reasoning output can be expressed as follows,

$$\begin{aligned}\mu_{D_o}(\eta) = \big(&\mu_{A_1}(\gamma_1)\wedge\mu_{B_1}(\gamma_2)\wedge\mu_{C_1}(\gamma_3)\wedge\mu_{D_1}(\eta)\\ &\vee\mu_{A_2}(\gamma_1)\wedge\mu_{B_2}(\gamma_2)\wedge\mu_{C_2}(\gamma_3)\wedge\mu_{D_2}(\eta)\\ &\vee\mu_{A_3}(\gamma_1)\wedge\mu_{B_3}(\gamma_2)\wedge\mu_{C_3}(\gamma_3)\wedge\mu_{D_3}(\eta)\\ &\cdots\\ &\vee\mu_{A_n}(\gamma_1)\wedge\mu_{B_n}(\gamma_2)\wedge\mu_{C_n}(\gamma_3)\wedge\mu_{D_n}(\eta)\big)\end{aligned} \tag{6}$$

where $\wedge$ is the minimum operation, and $\vee$ is the maximum operation, respectively.

The defuzzified output η_o is calculated using the following equation [23],

$$\eta_o = \frac{\Sigma \eta \mu_{D_o}(\eta)}{\Sigma \mu_{D_o}(\eta)} \tag{7}$$

4.1. Application of The Fuzzy Inference System

Three input values and one output value, among the different shapes of fuzzy set are present in this investigation. The input variables are Low (L), Medium (M), and High (H) and the output variables are stated as five membership functions such as Very Low (VL), Low (L), Medium (M), High (H), and Very High (VH). Thus, the fuzzy rule base which has twenty-seven rules is presented in Table 8.

Table 8. *Fuzzy rule base*

T_{avg} (Low)		**T_{rip}**		
		Low	Medium	High
THD	Low	VL	VL	L
	Medium	VL	L	M
	High	L	M	H

T_{avg} (Medium)		**T_{rip}**		
		Low	Medium	High
THD	Low	VL	L	M
	Medium	L	M	H
	High	M	H	VH

T_{avg} (High)		**T_{rip}**		
		Low	Medium	High
THD	Low	L	M	H
	Medium	M	H	VH
	High	H	VH	VH

Fuzzy inference system is used for solving interrelationships among multiple response. In this approach a multi-response performance index (MRPI) is obtained for analyzing complicated the multiple response. The FIS implementation steps are summarized below.

Step 1. The S/N ratios corresponding to three responses (T_{avg}, T_{rip} and THD) are calculated using Eqs. 2 and 3 in the Minitab software. The average torque is investigated for the LIB condition, whereas the torque ripple and THD are investigated for the SIB condition. These values are given in Table 9.
Step 2. Gaussian membership function and fuzzy rules are established to fuzzify the S/N ratio of each response. These functions and rules are given in Figure 7 and Table 8, respectively.
Step 3. The fuzzy multi-response output is calculated using the max-min interface operation (Eq. 6)
Step 4. A single response multi-response performance index (η_o), in which case the optimal design variables is calculated using Eq. 7 and given with the S/N ratios in Table 9. Fuzzy Logic Toolbox of Matlab software was used for the stage 2–4.
Step 5. The multi-response performance index is analyzed using the Taguchi method again to determine new optimal design variables. The values and the main effects of the multi-response performance index are shown in Table 10 and Figure 8, respectively.

Table 9. *Responses for the fuzzy inference system*

	S/N			MRPI
n	**T_{avg}**	**T_{rip}**	**THD**	**-**
1	23.6768	-10.5783	-1.9382	0.878
2	22.9905	-12.4235	-1.5109	0.674
3	21.7343	-15.534	-1.214	0.636
4	20.9921	-14.5671	-2.1442	0.408
5	23.137	-14.083	-1.2892	0.725
6	22.9535	-11.0534	-1.5109	0.763
7	20.9377	-13.9271	-2.0761	0.402
8	22.6772	-12.8493	-1.5109	0.666
9	18.8103	-19.6364	-2.4115	0.113
10	22.6963	-12.7698	-2.9844	0.376
11	22.4049	-13.122	-3.3464	0.295
12	23.8402	-10.8066	-2.8603	0.736
13	23.2094	-11.7092	-2.9226	0.554
14	23.2034	-10.9801	-3.1673	0.624
15	20.9999	-13.8569	-3.2274	0.295
16	22.8603	-11.9758	-3.5218	0.432
17	18.978	-17.1828	-3.8625	0.121
18	20.9999	-12.2132	-3.2274	0.375

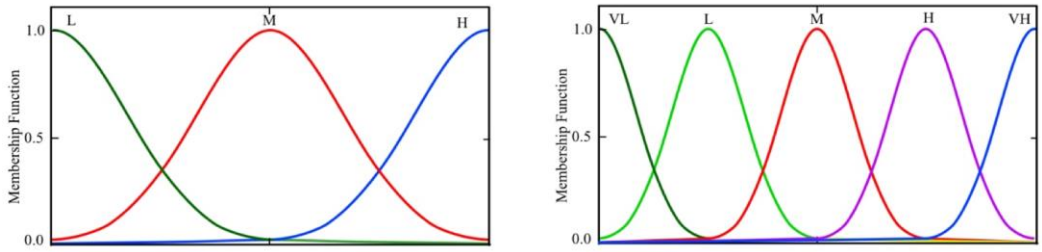

(a) The S/N ratios of T_{avg} [18.81;23.84], T_{rip} [-19.64;-10.58], and THD [-3.86;-1.21]

(b) The MRPI [0;1]

Figure 7. *Membership functions for a) one of three inputs and b) one output*

Table 10. *MRPI for the design variables*

Level	**A**	**B**	**C**	**D**	**E**	**F**	**G**
i=1	0.6584	0.6957	0.6175	0.4192	0.6393	0.6753	0.6212
i=2	0.5284	0.6572	0.5910	0.6960	0.6190	0.5290	0.5472
i=3	-	0.4275	0.5718	0.6652	0.5220	0.5760	0.6120
LIB	A1	B1	C1	D2	E1	F1	G13

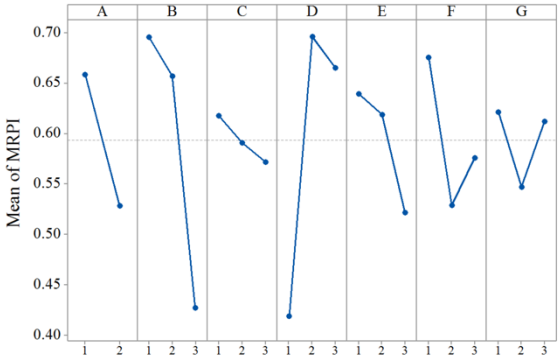

Figure 8. *Effect of main design variables on multi-response performance index*

4.2. Optimal Design Variables for The Fuzzy Inference System

As a result of the fuzzy on based the Taguchi analysis, the design variables can be divided into three groups in terms of their variations. The first group consists of magnet thickness (B) and rotor height (D), and has the most effective multi-response. The second group consists of magnet embrace (A), slot-opening width (E), slot-opening height (F), and has a very effective multi-response.

According to the fuzzy based on the Taguchi method, the optimal combination of design variables is A1-B1-C1-D2-E1-F1-G13. Both G1 and G3 were tried for obtaining optimal variable values because design-variable G has a similar value for the two cases (G1, G3). The responses that correspond to the optimal design variables are given with two combinations in Table 11. The first combination is the same as the third solutions of the Taguchi analysis. The improvement in average torque, torque ripple, and back EMF THD are 20.3%, 32.8%, and 25.2%, respectively.

Table 11. *Responses for the fuzzy based the Taguchi method*

Model	**T_{avg} (Nm)**	**T_{rip} (%)**	**THD (%)**
Reference	12.55	5.15	1.63
1: A1-B1-C1-D2-E1-F1-G1	15.10	3.46	1.22
2: A1-B1-C1-D2-E1-F1-G3	13.92	3.50	1.17
Improvement in # 1	20.3%	-32.8%	-25.2%
Improvement in # 2	10.9%	-32.0%	-28.2%

5. OPTIMIZATION WITH GENETIC ALGORITHM

Genetic algorithms (GAs) are well-known types of evolutionary estimate methods, and they have been adapted for many applications in different fields. The GAs differ from most optimization methods because of their global seeking from one population of solutions rather than from one single solution. Non-dominated sorted genetic algorithm II (NSGA-II) is used to solve the constrained multi-objective optimization problem. It can be inferred that NSGA-II is very effective in solving multi-objective optimizations. Two distinguishing features of NSGA-II are its speed of convergence and good uniform distribution [24,25].

The GA is a heuristic method inspired by the natural biological evolutionary process including of a fit selection, crossover, mutation, etc. The GA schema is given in Figure 9.

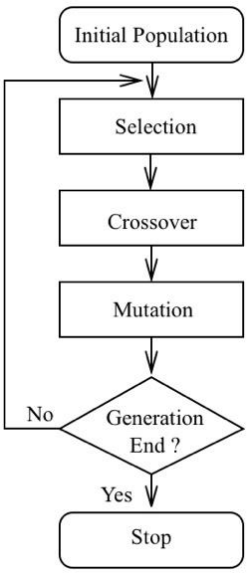

Figure 9. *General schema of genetic algorithm*

A multiobjective optimization problem (MOP) can be stated as follows:

$$\begin{aligned} &\text{minimize} \quad F(x) = \left[f_1(x), \ldots, f_{\mathrm{m}}(x) \right] \\ &\text{subject to} \quad \mathrm{x} \in \Omega \end{aligned} \tag{8}$$

where Ω is the decision (variable) space, $F : \Omega \to R^m$ consists of m real-valued objective functions and R^m is called the objective space. The attainable objective set is defined as the set $\{F(x) \mid x \in \Omega\}$. If $x \in \mathrm{R}^{\mathrm{n}}$, all the objectives are continuous and Ω is described by,

$$\Omega = \{ x \in R^n \mid h_j(x) \le 0, j=1,\ldots,m \} \tag{9}$$

where h_j are continuous functions, we call (Eq. 8) a continuous MOP [24,26].

There are a set of global optimal solutions, called a Pareto-optimal solution set in a MOP. All non-dominated solutions are the optimal solutions of the problem. These solutions set is named Pareto set while its image in objective space is named Pareto front.

Let $u = (u_1, \ldots, u_m)$, $v = (v_1, \ldots, v_m) \in R^m$ be two vectors, u, is said to dominate v if $u_i \le v_i$ for all $i=1,\ldots,m$ and $u \ne v$. A point $x^{\mathrm{å}} \in R^m$ is called (globally) Pareto optimal if there is no $x \in \Omega$ such that $F(x)$ dominates $F(x^{\mathrm{å}})$. The set of all the Pareto optimal points, denoted by Pareto set. The set of all the Pareto objective vectors, $PF = \{ F(x) \in R^{\mathrm{m}} \mid x \in PS \}$ is called the Pareto front [24,26].

5.1. Application of The Genetic Algorithm Method

It is assumed that the multi-objective optimization problem has following design variables in this study,

$$x = \left[E_m, T_m, O_m, H_{\mathrm{r}}, b_{\mathrm{s0}}, h_{\mathrm{s0}}, g \right] \tag{10}$$

The design variables are constrained by reasonable lower and upper bounds,

$$\begin{aligned} Bound_{lower} &= [0.88, \quad 8, 12, 12, 2.6, 0.4, 0.45] \\ Bound_{upper} &= [0.90, 10, 16, 14, 2.8, 0.6, 0.55] \end{aligned} \tag{11}$$

In the first method, three objective functions are considered separately. Multiple regression analysis is conducted to determine objective functions for each response using the $L18$ response values using Minitab software (Table 4). The three objective functions T_{avg}, T_{rip}, THD correspond to maximization of the average torque, minimization of the torque ripple and the back-EMF THD, respectively. The objective functions are expressed as follows:

$$T_{avg} = 17.37 + 0.209A - 1.375B - 0.554C + 1.114D - 0.588E - 0.487F - 0.529G \tag{12}$$

$$T_{rip} = 2.62 + 0.724A + 0.695B + 0.479C - 0.767D + 0.999E + 0.296F - 0.069G \tag{13}$$

$$THD = 1.0506 + 0.23A + 0.0358B - 0.0133C - 0.0375D - 0.0058E + 0.0017F - 0.01G \tag{14}$$

The multi-objective optimization problem can be stated as:

$$F = \left[T_{rip}(x),\ -T_{avg}(x),\ -THD(x) \right] \tag{15}$$

A multi-objective optimization was performed using multi-objective genetic algorithm in Optimization Toolbox of Matlab software. Since both functions are intended to be minimized, the average torque was multiplied by –1. The GA parameters selected were as follows, population size (s_p=3000), number of generations (n_g=200), probability of mutation (p_m=0.008), cross over rate (r_{co}=0.5), selection function (tournament), crossover function (scattered) and mutation function (adaptive feasible). The optimal value is obtained after 133 generations.

The set of solutions is also known as a Pareto front. Figure 10 shows the Pareto front obtained for the two objective function pairs, the average torque & the torque ripple and the average torque & THD. The average torque is directly proportional to the torque ripple, whereas it is inversely proportional to THD. Although all the points in this Pareto front are optimal points, the three selected points which have been assigned as Points A, B and C were chosen as the sample.

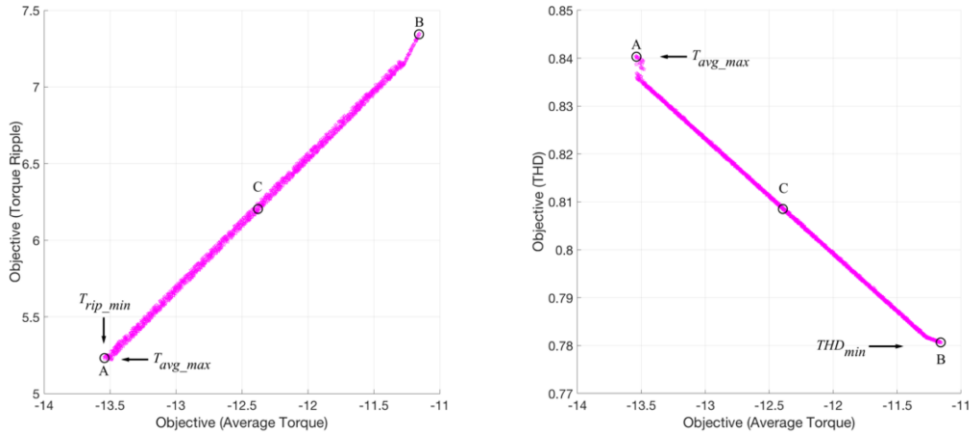

Figure 10. *Pareto front of average torque vs. torque ripple and THD*

The combination of design variables corresponding to point A, B, and C are A1-B1-C1-D3-E1-F1-G1, A1-B1-C3-D3-E1-F1-G3, and A1-B1-C2-D3-E1-F1-G2, respectively. Thus, the optimal combination was obtained for the GA based the Taguchi method as A1-B1-C1-D3-E1-F1-G1.

The second method has been implemented by converting the three objective functions into a single MRPI function. MRPI regression equation, which is named as fitness function, has been obtained using the MRPI response values in Minitab software (Table 9).

$$MRPI = -1.082+0.13A+0.1341B+0.0228C-0.123D+0.0587E+0.0497F+0.0046G \tag{16}$$

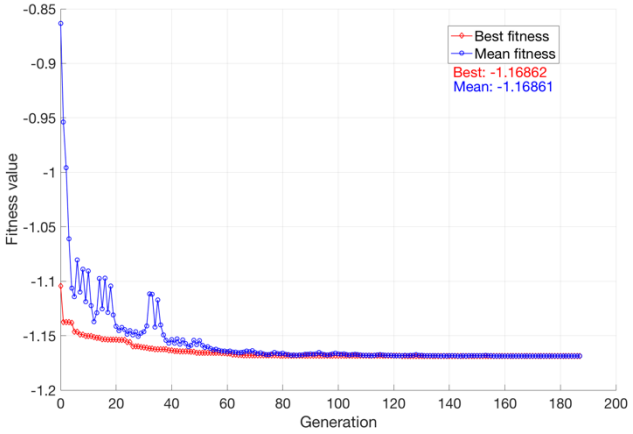

Figure 11. *Best fitness for fitness function of MRPI variation*

The best fitness value (γ = -1.16862) was resulted and final parameters were reached for GA. Figure 11 shows the best and the mean fitness of fitness function after 130 generations. Unlike the multi-objective optimization based GA, this genetic algorithm method gives a single optimal combination whose value was A1-B1-C1-D3-E1-F1-G1 for the GA based Fuzzy–Taguchi method.

The same optimal combination was obtained as a result of the above two genetic analyzes. This combination is the same as the fourth solutions of the Taguchi analysis (Table 7), whereas it differs from the results of the fuzzy based the Taguchi analysis (Table 11). Average torque, torque ripple, and back-EMF THD are obtained at 14.02 Nm, 3.94% and 1.24%. The improvement in average torque, torque ripple, and back EMF THD are 11.2%, 23.5%, and 23.9%, respectively, for the GA with the Taguchi and the FIS.
Although the combinations of the FIS and the GA are slightly different, the multi-response values are close to each other. The first one uses the membership function and the second one uses the regression equation, which is the likely reason.

6. CONCLUSION

Excluding the stator height, seven design parameters were defined as design variables with optimal ranges. The magnet thickness (B) and rotor height (D) were identified as common high-impact design variables for the two responses of average torque and torque ripple. In addition, the slot-opening width (E) was found to be the most effective for minimizing the torque ripple.

The multi-response that consisted of the average torque, the torque ripple, and the THD was reduced to a single response (MRPI). Following this, the optimal design variables were obtained very quickly by using fuzzy inference system and genetic algorithm based on the Taguchi method. The optimal combination of design variables was obtained as A1-B1-C1-D2-E1-F1-G1 according to both the Taguchi method and the fuzzy analysis based on the Taguchi method. The improvement in average torque, torque ripple, and back EMF THD are 20.3%, 32.8%, and 25.2%, respectively.

However, the optimal combination obtained by the genetic algorithm differs from the previous one by D3. A considerable amount of multi-response improvements was achieved according to the results of the three optimizations.

In this study, an SPM machine with an outer rotor (OR) is selected for study. The geometry of this OR-SPM machine is shown in Figure 1, and its performance parameters are given in Table 1. These values are used as the multiple response/performance characteristics of the optimization process.

CONFLICTS OF INTEREST

No conflict of interest was declared by the authors.

REFERENCES

[1] Wu, D. ve Zhu, Z.Q., "Design Tradeoff Between Cogging Torque and Torque Ripple in Fractional Slot Surface-Mounted Permanent Magnet Machines", IEEE Transactions on Magnetics, 51(11): 1-4, (2015).

[2] Xu, Y., Zhao, J. ve Fu, X., "Quantitative Analysis for Influence of Structure Parameters on The Slot Harmonic in Fractional-Slot Permanent Magnet Motors", 17th International Conference on Electrical Machines and Systems, ICEMS 2014, Hangzhou, China, 349-353, (2015).

[3] Bianchi, N. ve Bolognani, S., "Design Techniques for Reducing the Cogging Torque in Surface-Mounted PM Motors", IEEE Transactions on Industry Applications, 38(5): 1259-1265, (2002).

[4] Huang, S., Zhang, J., Gao, J. ve Huang, K., "Optimization The Electromagnetic Torque Ripple of Permanent Magnet Synchronous Motor", International Conference on Electrical and Control Engineering, ICECE 2010, Wuhan, China, 3969-3972, (2010).

[5] Upadhayay, P. ve Rajagopal, K.R., "Torque Ripple Reduction Using Magnet Pole Shaping in A Surface Mounted Permanent Magnet BLDC Motor", 2nd International Conference on Renewable Energy Research and Applications, ICRERA 2013, Madrid, Spain, 516-521, (2013).

[6] Shen, Y. ve Zhu, Z.Q., "Analytical Prediction of Optimal Split Ratio for Fractional-Slot External Rotor PM Brushless Machines", IEEE Transactions on Magnetics, 47(10): 4187-4190, (2011).

[7] Tsai, W.C., "Robust Design of A 5MW Permanent Magnet Synchronous Generator Using Taguchi Method", 7th International Conference on Computing and Convergence Technology, ICCCT 2012, Seoul, South Korea, 1328-1334, (2012).

[8] Kim, S.I., Lee, J.Y., Kim, Y.K., Hong, J.P., Hur, Y. ve Jung, Y.H., "Optimization for Reduction of Torque Ripple in Interior Permanent Magnet Motor by Using The Taguchi Method", IEEE Transactions on Magnetics, 41(5): 1796-1799, (2005).

[9] Sujin, L., Kyuseob, K., Sugil, C., Junyong, J., Taehee, L. ve Jungpyo, H., "Optimal Design of Interior Permanent Magnet Synchronous Motor Considering The Manufacturing Tolerances Using Taguchi Robust Design", Electric Power Applications, IET, 8(1): 23-28, (2014).

[10] Chang-Chou, H., Chia-Ming, C. ve Ping-Lun, L., "Design Optimization for Cogging Torque Minimization and Efficiency Maximization of A High-Speed PM Motor", International Conference on Power Electronics and Drive Systems, PEDS 2009, Taipei, Taiwan, 938-943, (2009).

[11] Gaing, Z.L. ve Chiang, J.A., "Robust Design of In-Wheel PM Motor by Fuzzy-Based Taguchi Method", IEEE Power and Energy Society General Meeting, Michigan, USA, 1-7, (2010).

[12] Hwang, C.C., Chang, C.M. ve Liu, C.T., "A Fuzzy-Based Taguchi Method for Multiobjective Design of PM Motors", IEEE Transactions on Magnetics, 49(5): 2153-2156, (2013).

[13] Gaing, Z.L., Wang, Q.Q. ve Chiang, J.A., "Optimization of In-Wheel PM Motor by Fuzzy-Based Taguchi Method", International Power Electronics Conference, IPEC 2010, Singapore, Singapore, 1312-1316, (2010).

[14] Bianchi, N. ve Bolognani, S., "Design Optimisation of Electric Motors by Genetic Algorithms", IEE Proceedings-Electric Power Applications, 145(5): 475-483, (1998).

[15] Hwang, C.C., Lyu, L.Y., Liu, C.T. ve Li, P.L., "Optimal Design of An SPM Motor Using Genetic Algorithms and Taguchi Method", IEEE Transactions on Magnetics, 44(11): 4325-4328, (2008).

[16] Beniakar, M.E., Kakosimos, P.E., Krasopoulos, C.T., Sarigiannidis, A.G. ve Kladas, A.G., "Comparison of In-Wheel Permanent Magnet Motors for Electric Traction", 21st International Conference on Electrical Machines, ICEM 2014, Berlin, Germany, 2472-2478, (2014).

[17] Chowdhury, M., Islam, M., Gebregergis, A. ve Sebastian, T., "Robust Design Optimization of Permanent Magnet Synchronous Machine Utilizing Genetic and Taguchi's Algorithm", IEEE Energy Conversion Congress and Exposition, ECCE, Denver, USA, 5006-5012, (2013).

[18] Woo, D.-K., Kim, I.-W. ve Jung, H.-K., "Optimal Rotor Structure Design of Interior Permanent Magnet Synchronous Machine based on Efficient Genetic Algorithm Using Kriging Model", Journal of Electrical Engineering and Technology, 7(4): 530-537, (2012).

[19] Rostami, N., Feyzi, M.R., Pyrhonen, J., Parviainen, A. ve Behjat, V., "Genetic Algorithm Approach for Improved Design of A Variable Speed Axial-Flux Permanent-Magnet Synchronous Generator", IEEE Transactions on Magnetics, 48(12): 4860-4865, (2012).

[20] Krishnaiah, K. ve Shahabudeen, P., Applied Design of Experiments and Taguchi Methods, PHI Learning Pvt. Ltd., (2012).

[21] Zadeh, L.A., "Fuzzy Sets", Information Control, 8(3): 338–353, (1965).

[22] Mamdani, E.H. ve Assilian, S., "An Experiment in Linguistic Synthesis with A Fuzzy Logic Controller", International journal of human-computer studies, 51(2): 135-147, (1999).

[23] Jang, J.S.R., Sun, C.T. ve Mizutani, E., Neuro-Fuzzy and Soft Computing: A Computational Approach to Learning and Machine Intelligence, Prentice-Hall Inc., (1997).

[24] Srinivas, N. ve Deb, K., "Muiltiobjective Optimization Using Nondominated Sorting in Genetic Algorithms", Evolutionary Computation, 2(3): 221-248, (1994).

[25] Deb, K., Pratap, A., Agarwal, S. ve Meyarivan, T., "A Fast and Elitist Multiobjective Genetic Algorithm: NSGA-II", IEEE Transactions on Evolutionary Computation, 6(2): 182-197, (2002).

[26] Li, H. ve Zhang, Q., "Multiobjective Optimization Problems with Complicated Pareto Sets, MOEA/D and NSGA-II", IEEE Transactions on Evolutionary Computation, 13(2): 284-302, (2009).